Measurement of total pressure, static pressure and wind velocity around cross-ventilated building

N. Nishimoto, K. Sagara, T. Yamanaka, H. Kotani, and T. Kobayashi

Osaka University

S. Takeda

Nikken Sekkei. Ltd.

ABSTRACT

Conventionally, the flow rate of a cross-ventilated building is predicted by using the orifice equation. When the opening is small, flow becomes like infiltration through cracks, it is useful. However, the flow rate could be underestimated when the orifice equation is applied to the cross-ventilated flow through large openings. The goal of this research is to propose the prediction method of the flow rate of a cross-ventilated building by considering the power balance inside the whole stream tube. It is needed to know the properties of the flow field, but few measurements of the pressure or the wind velocity around a cross- ventilated building have been conducted. To reveal the properties of the flow around a cross- ventilated building, the wind tunnel test was conducted.

The studied model in this paper has the rectangular configuration provided with two openings on the opposite sides. The opening size and the model depth were set up as the parameter. This paper presents the experimental results of the wind velocity measured by Particle Image Velocimetry (PIV) system, and the total/static pressure measured by the pressure tube around the cross-ventilated building. Finally, differences in characteristics of the flow field will be shown.

1. INTRODUCTION

Cross-ventilation is beneficial to save energy and obtain thermal comfort in a hot summer. In predicting the flow rate of a cross-ventilated building, the orifice equation is usually used, where the discharge coefficients obtained from the chamber method and the wind pressure coefficient from a sealed building are applied. However, this method could underestimate the flow rate of the building if the openings are large as shown in Ishihara (1969).

Many studies about this problem have conducted for a long time. As an alternative method, Murakami and Kato et al. (1991, and 2004) introduced the power balance model, where flow rate is predicted based on the energy conservation inside the stream tube passing through/around the building, as this idea was originally introduced by Guffy et al. (1989). Here, the stream tubes are divided into the control volumes. The transported power (Transported energy rate [J/s=W]) on the inlet section of a control volume is balanced with that on the outlet section and the power loss inside the control volume. This method could be appropriate even for buildings provided with large openings. In order to predict the flow rate, the power losses inside the stream tubes are needed to be predicted. However, the details of the transported power and the power loss inside the stream tubes have not been published yet. Therefore, the authors aim to clarify the basic tendencies of the pressures and the velocity inside the stream tubes, which are needed for calculating the transported power.

Many wind tunnel measurements for the velocity field inside/outside of the building and the pressure on the wall surface have been conducted so far. For example, Jiang et al. (2003) measured the velocity around a cross-ventilated building model and Murakami et al. (1991) measured the distributions of floor surface pressures. However, few works dealt with the measurement of the spatial total/static

pressure. This must be investigated to consider the power balance of the stream tube. The authors have shown the total/static pressure distributions along the centerline of the stream tube passing through a cross-ventilated building model by conducting the wind tunnel experiment (See Kobayashi et al. (2006)). In this paper, the stream tubes passing around the building model are focused, and the total/static pressures are measured. These pressures are to be measured by orienting a pressure tube to the wind direction. Therefore, the wind direction is needed to be known beforehand. In this study, the velocity distributions around the building model were measured by using the PIV system mainly in order to obtain the flow direction for the pressure measurement. Based on these angles, the spatial total/static pressures are measured by rotating the pressure tube.

2. Velocity Measurement by PIV System

This chapter describes the distributions of the wind velocity around the model by using the PIV system and the results of the velocity are shown in two forms. The results of the wind velocity will be used in the next chapter where the pressures around the model are measured with pressure tubes because the wind direction needs to be known for each measuring point.

2.1 Experimental Setup

2.1.1 Model and Cases

The geometrical shape of the room model used in this study is depicted in Fig. 1. The model depth (D) and the opening size (L) are inside dimensions. For all cases, models have the side walls of which thickness is 6.0 mm and the end walls of which thickness is 3.0 mm. All walls are made of acrylic board. On the side walls, there are grooves of 1 mm width and 1 mm depth every 30 mm in X direction in order to make it possible to set partitions provided with an opening, though those partitions were not used in this study. For the parametric analysis, D and L were changed as shown in Fig. 2.

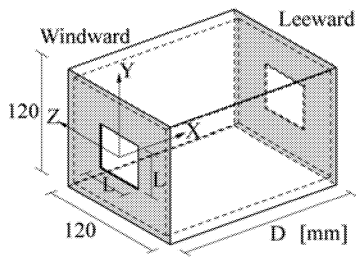

Fig. 1: Geometry of studied model

2.1.2 Facilities

The closed-circuit type wind tunnel of Osaka University (Osaka, Japan) is used. It has a test section of 1.8 m width, 1.8 m height and 9.5 m length. Fig. 3 shows the cross sections of the wind tunnel. The room model was set on the center of Y-Z section of the wind tunnel with its opening perpendicular to the approaching flow. The visualization by tracer injection method was conducted under a uniform approaching flow of 10 m/s. The smoke was generated by a smoke generator and injected to the upstream of the model by using a compressor. A double pulse Nd: YAG laser (KANOMAX) was used as a light source and a laser sheet was oriented horizontally across the model. Flow Master System (La Vision) is used as the PIV system. A high-speed camera was set above the model. A pair of pictures was taken 100 times with a time interval of 100 μs at the frequency of 4Hz. As the image processing program of the PIV, Davis 7.2 (La Vision) was used. As a PIV algorithm, FFT cross-correlation method was used.

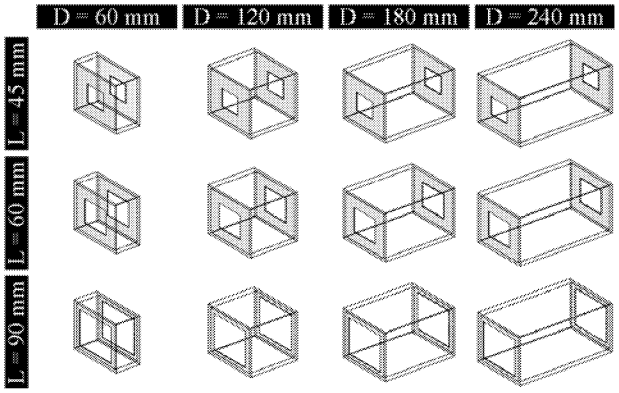

Fig. 2: Studied cases for measurement

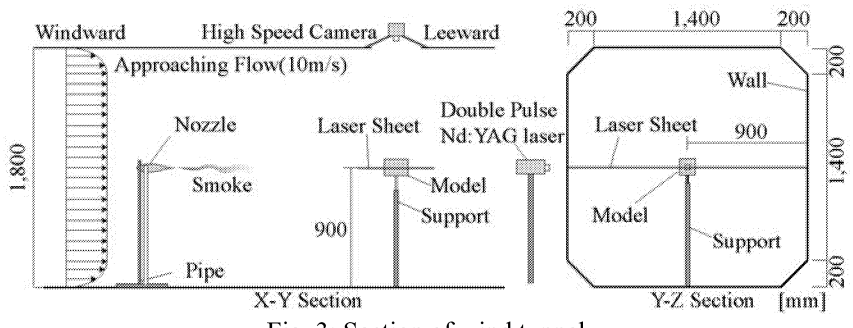

Fig. 3: Section of wind tunnel

2.2 Results and Discussions

Fig. 4 shows the velocity distributions on the central cross section (Y=0) as two dimensional average velocity vector. Fig. 5 shows the contour lines for the velocity scalar. In the case of large openings, larger angle of separation and larger low-velocity region around the model can be seen if compared to the case of small openings with the same model depth. This is because the flow does not enter through the small opening easily and it flows along the wall. Therefore, Z component of the velocity becomes large. Regarding the cases of D=180, 240 mm, the reattachment of the separating flow

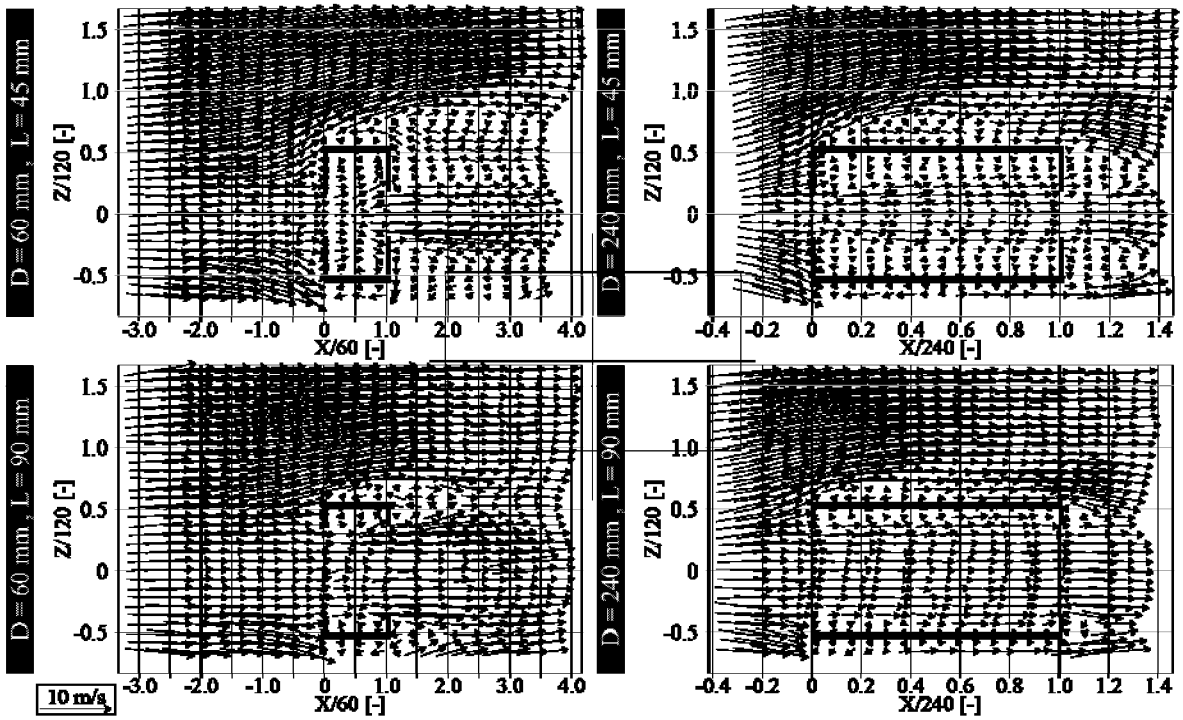

Fig. 4: Vector of velocity

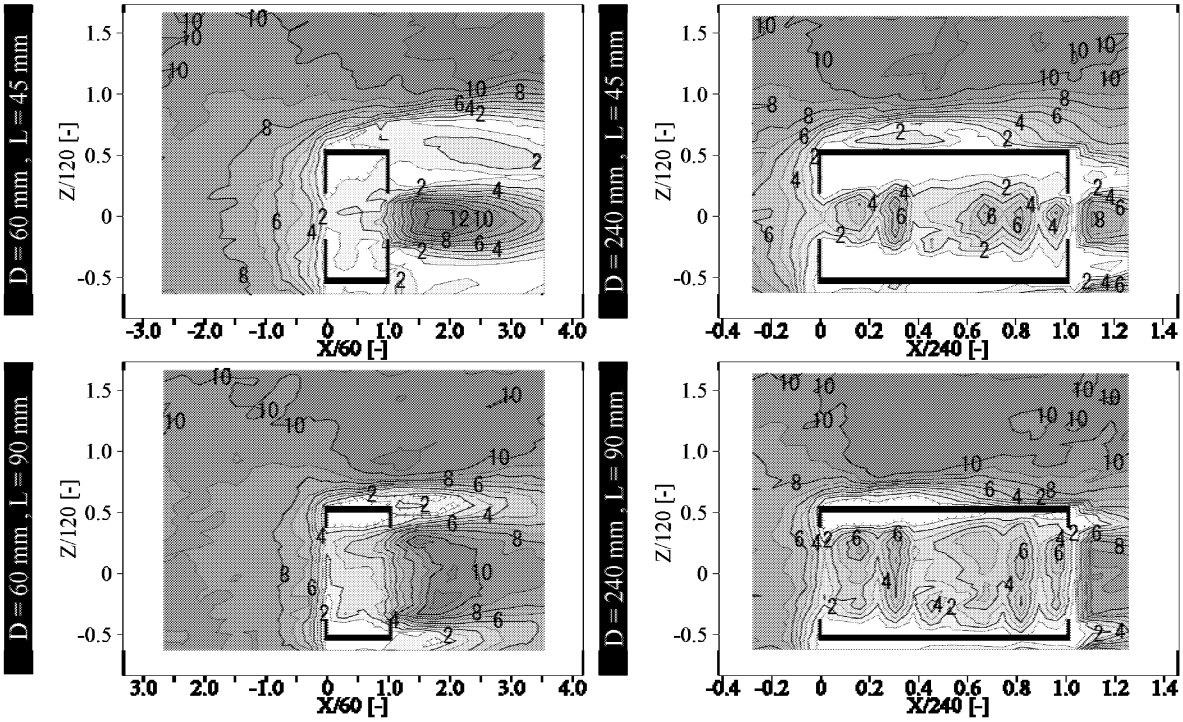

Fig. 5: Contour line for velocity scalar

to the side wall can be seen. This tendency is different from that in the cases of D=60, 120 mm, and is thought to cause larger energy loss. On the leeward region of the leeward opening, the velocity becomes large as the model becomes small in the cases of the same opening size. Because the laser light was reflected on the groove and the movement of the smoke was not detected accurately in computing the velocity, the velocity inside the model is underestimated.

3. Pressure Measurement with Pressure Tubes

In order to understand the energy transport and dissipation around the model, the total and static pressure around the model were investigated by using the pressure tubes based on the wind direction obtained from the PIV measurement. The velocity distribution calculated from the dynamic pressure is also shown.

3.1 Experimental Setup

3.1.1 Facilities

The experiment was conducted by using the same wind tunnel as illustrated in Chapter 2. Fig. 6 shows the coordinate axis and the basic measuring points. As shown in Fig. 7, the pressure tube with protractor was attached to the aluminum square pipe fixed to the 3-D traverser hung from the ceiling. Fig. 8 shows the details of the pressure tubes. The total and static pressure around the model were measured by a pressure transducer (VARIDYNE, MP45-14) under a uniform approaching flow of 10 m/s. Fig. 9 shows the central section of the wind tunnel for the pressure measurement. The reference pressure was the static pressure obtained from the pitot tube shown in Fig. 9. The sampling frequency was 100 Hz and the averaging time was 30 seconds. Fig. 10 shows the directivities of the total and static pressure

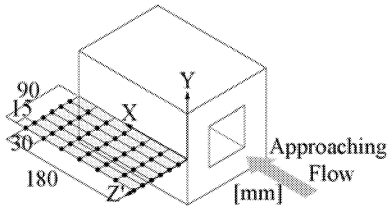

Fig. 6: Coordinate axis and basic measuring point

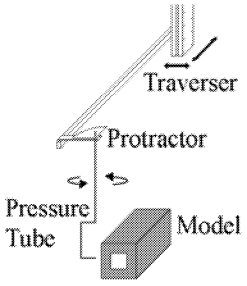

Fig. 7: Setting of measuring instrument

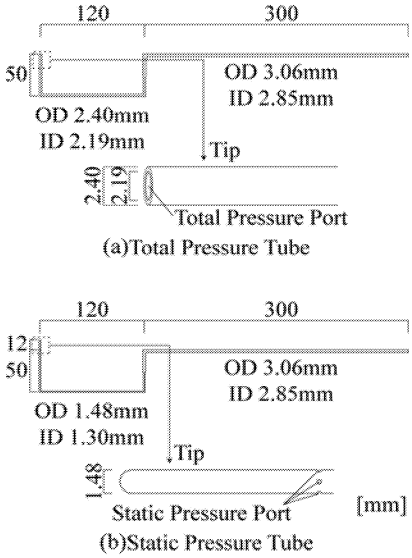

Fig. 8: Detail of pressure tube

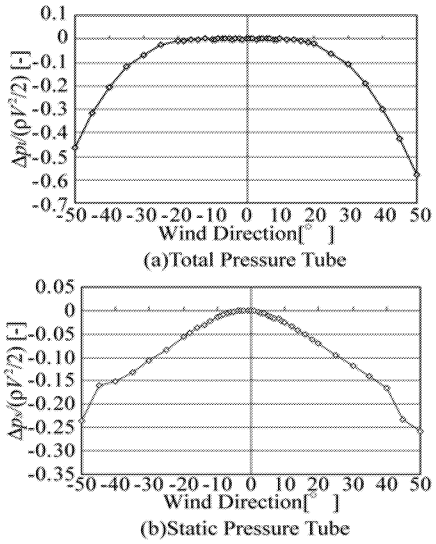

Fig. 10: Directivity of pressure tube

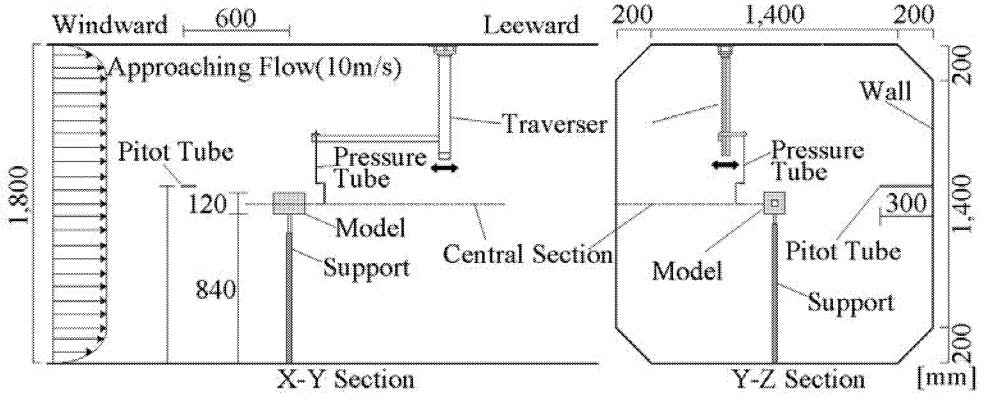

Fig. 9: Section of wind tunnel

tubes. These were measured separately without setting up the model. Assuming that the acceptable error was 2 %, the acceptable error in alignment of the total pressure tube and the static pressure tube were decided to be 18 deg. and 8 deg. respectively. Here the error is defined as the ratio of difference between measured pressure at 0 deg. and that at each wind direction (Δp_t , Δp_s) to the total pressure provided from the pitot tube. At each basic measuring point, the pressure was measured at the angles from +20 deg. to -20 deg. to the main wind direction obtained from the PIV measurement. The total pressure was measured at every 10 deg., and the static pressure, every 5 deg. In these measurements, the largest value of the pressure was adopted as the total and static pressure for each measuring point. After the initial measurements for the basic measuring points, new measuring points were added to the region where the total pressure gradient was large. The interval of additional measuring points is 5 mm in the Z direction.

3.1.2 Model and Cases

Although the geometrical shapes of the room model were the same as mentioned in Chapter 2 (See Fig. 1), the end walls were replaced by the brass walls of which thickness is 0.8 mm. The side walls were made of acrylic board and its thickness was 6.0 mm. For the parametric analysis, D was fixed at 180 mm and L was changed in three cases of 45, 60, and 90 mm.

3.2 Results and Discussions

Fig. 11 shows the total and static pressure distributions at each X-coordinate. Those pressures are normalized by dividing by the reference total pressure at the reference point of X=0 mm and Z'=90 mm. Fig. 12 shows the details of the measuring points. Z' is the distance from the side wall. At X=0 mm, though total pressures are almost constant at 1.0, static pressures decrease slightly near the side wall because of the contracted flow. In the region where X axis is more than 30 mm, decrease of the total pressure can be seen. For the cases of L=45, 60 mm, the difference between the total pressure and the static pressure rises sharply around Z'/120=0.17. As for the case of L=90 mm, this can be seen around Z'/120=0.14. In this region, therefore, it is thought that the gradient of the dynamic pressure is large and there is the separating boundary. Inside this boundary, for the cases of L=45, 60 mm, the total pressure and static pressure are almost equal in X=30-150 mm and for the case of L=90 mm, in X=60-120 mm. Therefore the velocity is thought to be very small. It was indicated in Chapter 2 that the smaller the opening is, the larger the low-velocity region around the model is. For this measurement, the smaller the opening is, the farther the location where the dynamic pressure varies sharply from the model.

Fig. 13 shows the velocity distributions calculated from dynamic pressure. Here it is easily seen that this low-velocity region becomes large in the case of small openings. This tendency corresponds to that of Chapter 2.

The gradient of the total pressure becomes smaller on the leeward region. Meanwhile the value of the total pressure around side wall rises. These results suggest that the energy is supplied from outside region of the separating boundary to inside. For all cases, the total pressures at Z'/120=0.5-0.75 show almost constant at 1.0. It can be said that the energy is mostly conserved in this region. Therefore, it is thought that the energy loss and the energy transportation occur inside the line of Z'/120=0.5.

4. CONCLUSIONS

From PIV measurement:

- In the case of small openings, the separation angle was large, but there weren't significant differences if the depth were varied.
- In the case of small openings, the low-velocity region around the model was large.

From pressure measurement:

- If the openings were small, the total pressure near the model was small.
- The gradient of the total pressure became smaller on the leeward region. Meanwhile the value of the total pressure around side wall rose.
- The energy loss and the energy transportation are expected to occur on the inside Z'/120=0.5.
- The velocity distributions obtained from the pressure measurement were similar to those obtained from PIV measurement.

ACKNOWLEDGEMENT

The PIV measurement was supported by Mr. Yasuhiro Shiozaki and Ms. Yasue Tanaka, KANOMAX JAPAN, INC. and this is gratefully acknowledged.

REFERENCES

Ishihara M. (1969). Building Ventilation Design, Asakura Publisher. (In Japanese)

Guffy S.E., and Fraser D.A. (1989). A Power Balance Model of Converging and Diverging Flow Junctions. *ASHRAE Transactions*, Volume 95, pp.2-9.

Jiang Y. et al (2003). Natural ventilation in buildings: measurement in a wind tunnel and numerical simulation with large-eddy simulation, *Journal of Wind Engineering and Industrial Aerodynamics*, Volume 91, Number 3, pp.331-353.

Kato S. (2004). Flow Network Model based on Power Balance as Applied to Cross-Ventilation. *The International Journal of Ventilation*, Volume 2, Number 4, pp.395-408.

Kobayashi T. et al (2006). Wind Driven Flow through Openings – Analysis of the Stream Tube. *International Journal of Ventilation*, Volume 4, Number 4, pp.323-336.

Murakami S. et al (1991). Wind Tunnel Test on Velocity -Pressure Field of Cross-Ventilation with Open Windows, *ASHRAE Transaction*, Volume 97, Part1, pp.525-538

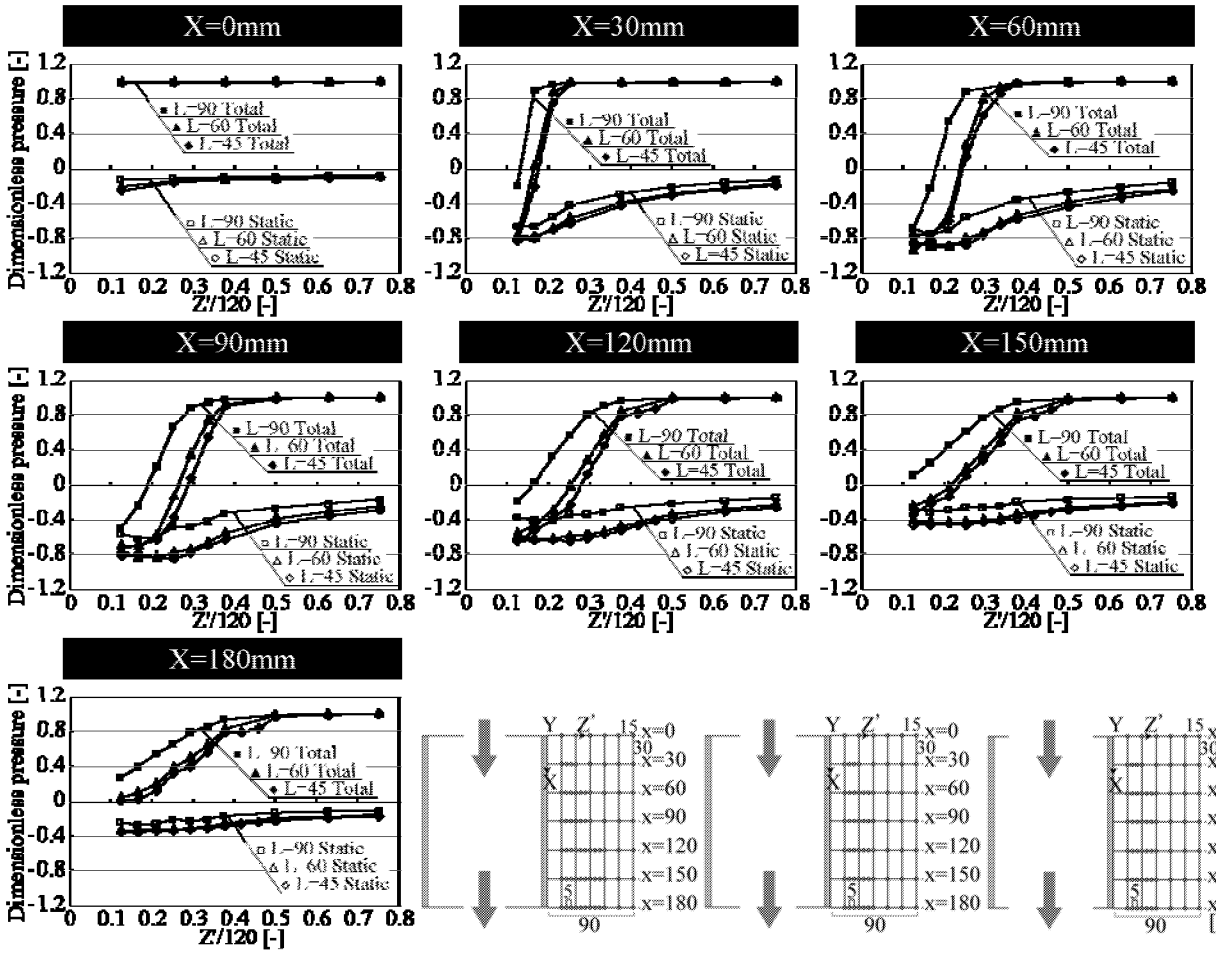

Fig. 11: Distribution of pressure

Fig. 12: Detail of measuring point

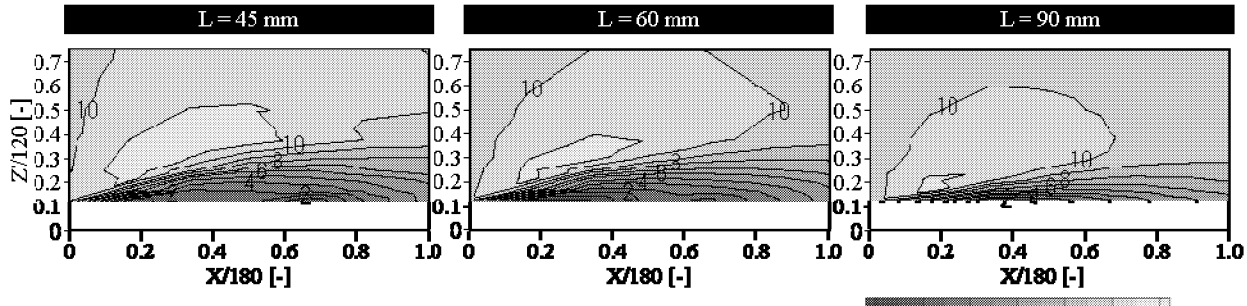

Fig. 13: Distribution of velocity